Impact of porous medium desiccation during anhydrous CO2 injection in deep saline aquifers: up scaling from experimental results at laboratory scale to near-well region

Laurent André, Mohamed Azaroual, Yannick Peysson, Brigitte Bazin

Impact of porous medium desiccation during anhydrous CO_2 injection in deep saline aquifers: up scaling from experimental results at laboratory scale to near-well region

Laurent André[a*], Mohamed Azaroual[a], Yannick Peysson[b], Brigitte Bazin[b]

[a]BRGM, Water Division, 3 Avenue Claude Guillemin, BP 36009, F-45060 ORLEANS Cedex 2 - France
[b]IFP, 1-4 avenue de Bois Préau, 92852 Rueil-Malmaison Cedex - France

---

Abstract

Injection of CO_2 in geological reservoirs or deep aquifers is nowadays studied to regulate the global warming by limiting the amount of greenhouse gases emitted by human activity into the atmosphere. CO_2 is captured from exhaust gas in power plants or industrial units and then stored in underground geological reservoirs. The experience available in the oil industry concerning CO_2 injection clearly shows that injectivity problems can occur due to several mechanisms like mineral dissolution but also physical alteration due to complete water desaturation of near wellbore through drying. This study presents experimental evaluations of drying of brine in sandstone samples and numerical modelling of the saturation profile evolution with two phase flow model integrating thermal effects. An up scaling/extrapolation of experimental results at laboratory scale to near-well zone is proposed highlighting the key role of injection flow rate and capillary properties on the desiccation mechanisms.

Keywords: supercritical CO_2, drying-out effects, coupled modelling, relative permeability.

---

1. Introduction

Geological sequestration of CO_2 into deep saline aquifers offers a promising solution for reducing net emissions of greenhouse gases into the atmosphere. Nevertheless, this emerging technology based on massive CO_2 injection in saline reservoirs can cause a major disequilibrium of the physical and geochemical characteristics of the host aquifer. Based on recent experiments and numerical simulations, the near-well injection zone is identified to be particularly impacted by supercritical CO_2 injection and the most sensitive area [1,2], where chemical (e.g., mineral dissolution/precipitation) and physical (e.g., temperature, pressure and gravity) phenomena have a major impact on the porosity and permeability and thus, at the end, on the well injectivity.

Among these perturbations, the desiccation of the porous medium appears as a major phenomenon with various implications as salts precipitation [3], modification of the local geomechanical constraints due to the salts precipitation, modification of internal forces and impact of injected fluids on the interfacial tensions including capillary/osmotic phenomena. Desiccation of porous media submitted to gas injections is a well-known process at the laboratory [4,5] and the field [6] scales. This process is taken into account only recently in the modelling of CO_2 storage in deep saline aquifers [1,7].

First, the massive and continuous injection of CO_2 in a saturated porous medium involves water displacement and evaporation: mobile water is removed by the injected supercritical CO_2 according to a two-phase system (brine – CO_2). At the end of this phase, immobile residual water, entrapped in pores or distributed on grain surface as a thin film, is in contact with the flowing dry CO_2 (i.e. with very low water vapour pressure). Consequently, a continuous and extensive evaporation process leads both to the apparition of a drying front moving into the medium, and the precipitation of salts and possibly secondary minerals in residual brines.

This study investigates the consequences on well injectivity of the porous medium desiccation through the petrophysical properties of different subsystems. This work is based on both experimental and numerical modelling approaches. Experimental evaluations of drying of brine are investigated at the laboratory scale on centimetre plugs of different materials. These experiments are then interpreted using a numerical modelling approach coupling hydraulic and thermal processes able to simulate the evolution of liquid and gas saturations in space and in time. A very fine discretization of the plugs allows capturing the continuous evolution of water and gas profiles in the porous medium and estimating the liquid saturation and the permeability evolution during drying process.

The parameters established at the centimetre scale are tentatively up scaled in order to extrapolate the results at the near wellbore scale and then, to forecast the impact of CO_2 injection on petrophysical properties of the host rock.

2. Experimental approach

The experiments of gas injection were performed on two materials:

- a low permeability sandstone ("Grès de Môlière" Φ=14.0 % and K_0=8 µD) in order to have a better experimental control of the pressure, to limit the gas flow rate and to increase the capillary effects that play a key role in drying processes,
- a "high" permeability sandstone ("Grès des Vosges" Φ=21.8 % and K_0=60 mD) in order to study rocks with properties close to the ones found in targeted reservoirs of CO_2 storage.

Sandstone samples of 6 cm long initially saturated with brine (salinity of 160 g L^{-1}) are placed in storage conditions (80°C-120°C – 50 bars) and in a cell transparent to X-ray. Dry gas (nitrogen) is injected in the fully saturated core plugs (Figure 1). Four long pressure stages are imposed to desaturate progressively the rock plug. The local water saturation in the sample is measured with X-ray attenuation techniques. Pressure difference and outlet gas flow rate are monitored during the experiment. The system evolves until complete drying. The experiments were performed at 90 and 120 °C with "Grès de Môlière" samples and at 90°C for "Grès des Vosges" core.

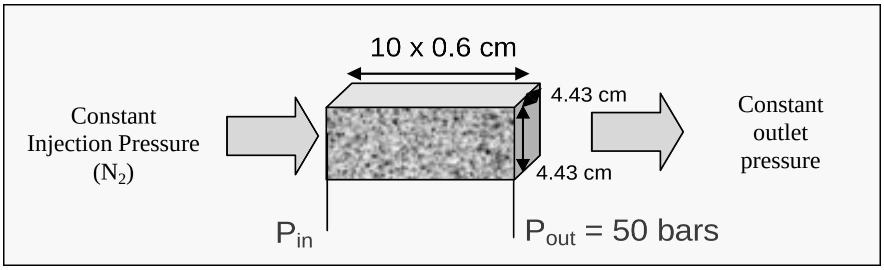

Figure 1 Experimental procedure to investigate the drying out of the core under a continuous flux of nitrogen.

3. Modelling approach

The TOUGH2 simulator [8] with the EOS7C module [9] was used for all the numerical simulations carried out for this study (core experiments and field scale). This code couples thermal and hydraulic processes and is applicable to one-, two-, or three-dimensional geologic systems with physical heterogeneity. The EOS7C is a fluid property module developed specifically to deal with mixtures of non-condensable gases (like CO_2 or N_2) and methane. It can be used to model isothermal or non-isothermal multiphase flow in water/brine/CH_4/(CO_2 or N_2) systems.

3.1. Modelling of core experiments with low permeability

Modelling approach consists to simulate the injection of nitrogen in a plug fully saturated with water. A two-phase Darcy flow is solved using relative permeability and capillary pressure curves. Thermodynamic equilibrium between concomitant phases (brine – N_2) is calculated at each time step to evaluate the water vapour fraction in the gas and the dissolved gas in the brine.

A 1D column model of 6 cm long is used as a conceptual framework for determining the evolution of the water content induced by the injection of N_2, in both time and space. The column is represented by 10 grid blocks composing the model mesh. The thickness of each grid cell is constant (0.6 cm). The rock constituting the matrix is supposed inert with respect to N_2, i.e. without chemical reactivity.

The variations of relative permeability and capillary pressure according to water saturation are given in Figure 2. Relative permeability for aqueous (k_{rl}) and gaseous (k_{rg}) phases and capillary pressure (P_{cap}) models are described according to the Van Genuchten formulation.

For the liquid phase:

$$k_{rl} = \sqrt{S^*}\left\{1-\left(1-\left[S^*\right]^{1/m}\right)^m\right\}^2 \quad \text{with} \quad S^* = \frac{S_l - S_{lr}}{1-S_{lr}}$$

where S_l is the liquid phase saturation, S_{lr} the residual liquid phase saturation and m a non-dimensional characteristic parameter of the law.

For the gas phase:

$$k_{rg} = \left(1-\hat{S}\right)^2.\left(1-\hat{S}^2\right) \quad \text{with} \quad \hat{S} = \frac{S_l - S_{lr}}{1-S_{lr}-S_{gr}}$$

where S_{gr} is the residual gas phase saturation.

Capillary pressure is calculated by the following expression:

$$P_{cap} = -P_0.\left(\left[S^*\right]^{-1/m}-1\right)^{1-m}$$

where P_o is the pressure coefficient in Pascal (Pa).

For “Grès de Môlière” rock, high pressure mercury injection and standard centrifugation have been done to measure the capillary pressure curve.

The model parameters are deduced: S_{lr} = 0.22, S_{gr} = 0.05, P_0 = 645161 Pa and m = 0.95.

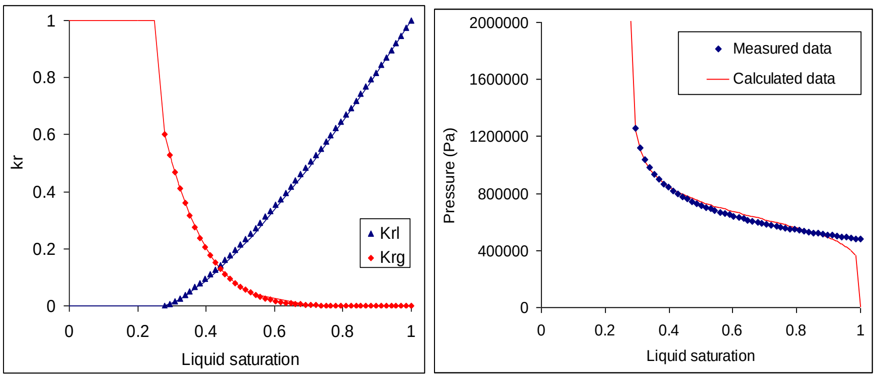

Figure 2 Relative permeability and capillary pressure curves according to liquid saturation (S_l).

3.2. Modelling of field experiments

A 1D radial model is proposed as a conceptual framework for determining the transient evolution of the water content induced by the injection of CO_2. The 1-m-thick reservoir is centred on a vertical injection well (Figure 3). The maximum radial extent is 100 km. Along the radius axis, the discretization is very fine close to the well (5 grid cells of 1 mm, then 5 grid cells of 2 mm, 77 grid cells of 5 mm and 960 grid cells of 10 mm up to 10 m from the injection well). 100 grid cells are assumed between 10 m and 100 m, 100 grid cells between 100 m and 10 km and 20 grid cells up to 100 km. In each interval (between 10 m and 100 km), the width of the radial elements follows a logarithmic scale. The objective of such refinement near the injection well is to capture more precisely both the details and the migration of the desiccation front in the near-well region.

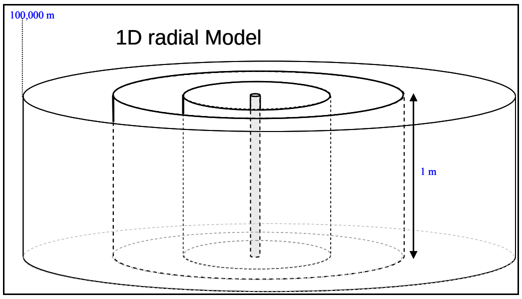

Figure 3 Geometrical 1D radial model for supercritical CO_2 injection.

No regional flow is considered and a hydrostatic status is initially assumed for the pressure within the reservoir and maintained constant at the lateral boundary. The initial temperature and pressure of the targeted reservoir are 80 °C and 240 bar, respectively.

The capillary pressure is determined experimentally with high pressure injection measurements. A standard Corey model is used for relative permeability curves of both liquid and gaseous phases whereas a Van Genuchten model is used to fit the experimental capillary pressure curve. For “Grès des Vosges” rock, $S_{lr} = 0.19$, $P_0 = 333\ 000$ Pa and m = 0.675 (Figure 4).

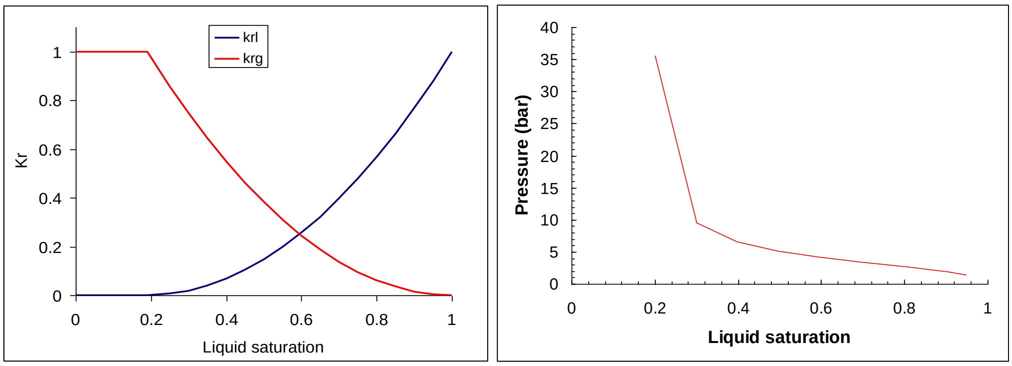

Figure 4 Relative permeability and capillary pressure curves according to liquid saturation (S_l).

4. Results

4.1. Modelling of core experiments

Three parameters have been followed during the experiments with “Grès de Môlière” rocks at 90°C:

- Mean water saturation in the core and outlet gas flow rate (Figure 5);
- The distribution of water content in the column (given by X-ray measurements) (Figure 6).

Due to the low permeability of the medium, we observe a very high sensitivity of the model to relative permeability and capillary pressure characteristics, in particular to the entry pressure. As shown by Figure 2, the Van Genuchten model does not fit properly the measured data when liquid saturation is close to 1. This very weak shift has an impact on the breakthrough time.

But, when this parameter is correctly defined, the code can reproduce, with a good agreement, the first 3 stages of the experiment including the mean water saturation and the outlet gas flow rate (Figure 5). These three first stages correspond to the desaturation of the porous medium according to a classical piston effect. The desaturation state is proportional to the pressure gradient applied to the core whereas the evaporation process is negligible: at the end of stage 3, the water content is close to the residual liquid phase saturation (Figure 6).

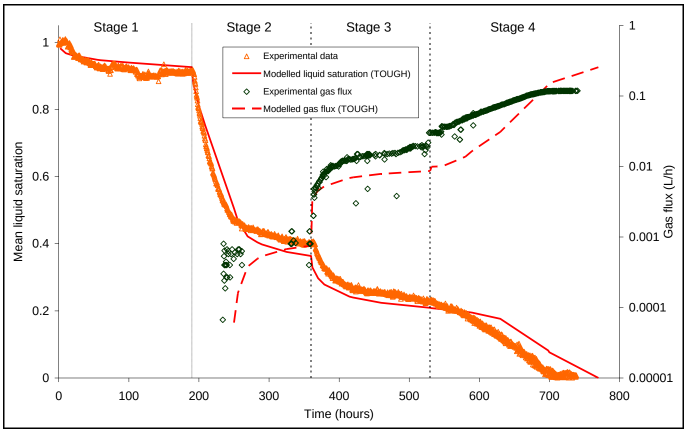

Figure 5 Variations of the mean water content in the core and outlet gas flux (experiment at 90°C): points are measured data whereas lines are calculated values.

During the first 3 stages, the calculated average water saturation in the core fit also the measured data (Figure 6). Some discrepancies are observed close to the inlet and the outlet of the column which are mainly due to the selected boundary conditions imposed to the numerical model.

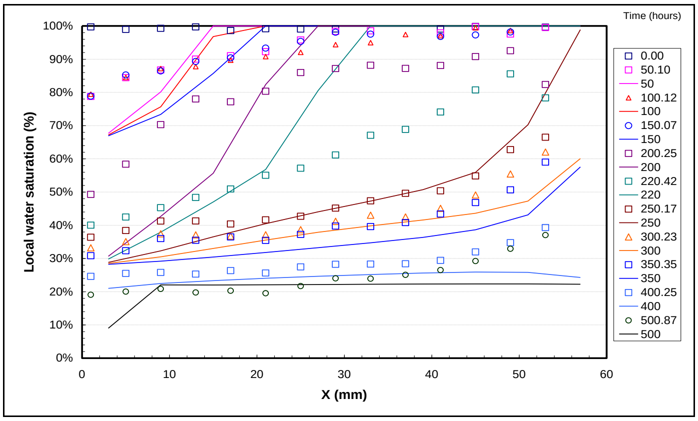

Figure 6 Variation of water content in the core (experiment at 90°C): points are measured data (X-ray measurements) whereas lines are calculated values.

The last stage (stage 4) corresponds to the real desiccation of the medium. Even if the global tendency is reproduced, this stage presented some difficulties to fit measured and calculated data. With the relative permeability curves shown in Figure 2, the calculated desiccation time was too long and the gas flow rate was underestimated.

Indeed, the only way to fit both gas flow rate and desiccation time (during stage 4) consists to increase the gas permeability when liquid saturation is lower than the residual liquid phase saturation. By increasing the relative gas permeability, the outlet gas flow rate is growing; the evaporation process goes faster and the time needed to totally desiccate the core decreases. Consequently, for $0 < S_l < 0.22$, k_{rg} is not threshold to 1: it follows a linear model with $k_{rg} = 20$ when $S_l = 0$ and $k_{rg} = 1$ when $S_l = S_{lr} = 0.22$.

These numerical simulations of laboratory experiments at 90°C allow checking the relevance of the model but also the determination of the most sensitive and ad hoc parameters of the integrated approaches (optimized relative permeability and capillary pressure curves). Then, from this set of parameters, we try to model the evaporation process on "Grès de Môlière" sample at 120°C. All the parameters established at 90°C are re-used for this test and obtained results are presented in Figure 7.

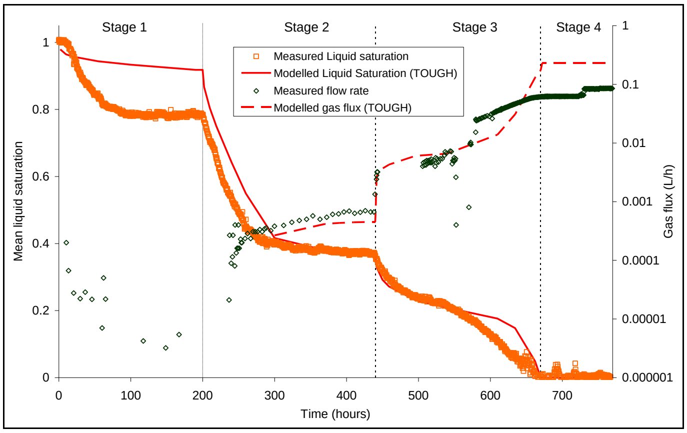

Figure 7 Variations of the mean water content in the core and outlet gas flux (experiment at 120°C): points are measured data whereas lines are calculated values.

The good coherence between measured and calculated data is very encouraging. We demonstrated that the petrophysical parameters established at 90°C are applicable to 120°C without any adjustment for the same rock.

4.2. Modelling at field scale

The same methodology as the one presented before was applied to "Grès des Vosges" sample. At laboratory scale, experiments of N_2 injection were performed to study the desiccation processes. Then a first modelling approach allowed defining the main parameters needed for field calculations (as capillary pressure and relative permeability curves). It is interesting to note here that no modification of gas relative permeability was necessary for this material. Because of the higher intrinsic permeability, the gas permeability does not have to be increased in order to satisfy the gas flow rate and the desiccation time. The k_{rg}-curve presented in Figure 4 is thus applied for field calculations.

The set of defined parameters is then applied to capture the behaviour of the near-well zone. Three scenarios were analysed:

- 1- A progressive increase of pressure to reach, at the end, a pressure gradient of 12 bar (in 3 stages);
- 2- A constant pressure gradient of 12 bar between the injection well and the reservoir pressure.
- 3- A constant pressure gradient of 24 bar between the injection well and the reservoir pressure.

In the scenario 1, the desaturation of the porous medium is progressive, in relation to the pressure stages imposed to the system. We observe nevertheless that the change of pressure is immediately followed by an abrupt decrease of water content before raising a plateau. Whatever the position with respect to the wellbore, the mechanisms of dessication are exactly the same and the values of the desaturation plateau are similar (Figure 8a). The last plateau of residual water amount (before total drying-out) is close to the value of the residual liquid phase saturation. Then, this water is evaporated by the gas flow.

In the scenario 2, the desaturation process is very fast (Figure 8b). But, the global mechanism is the same: water is removed from the porous medium, up to reach the residual liquid saturation. In a second step, the irreducible water is evaporated; this process is stopped by the total drying-out of the porous medium (Figure 8b). The scenario 3 presents the same results as the second one. Always the same amount of water is evaporated (Figure 8c).

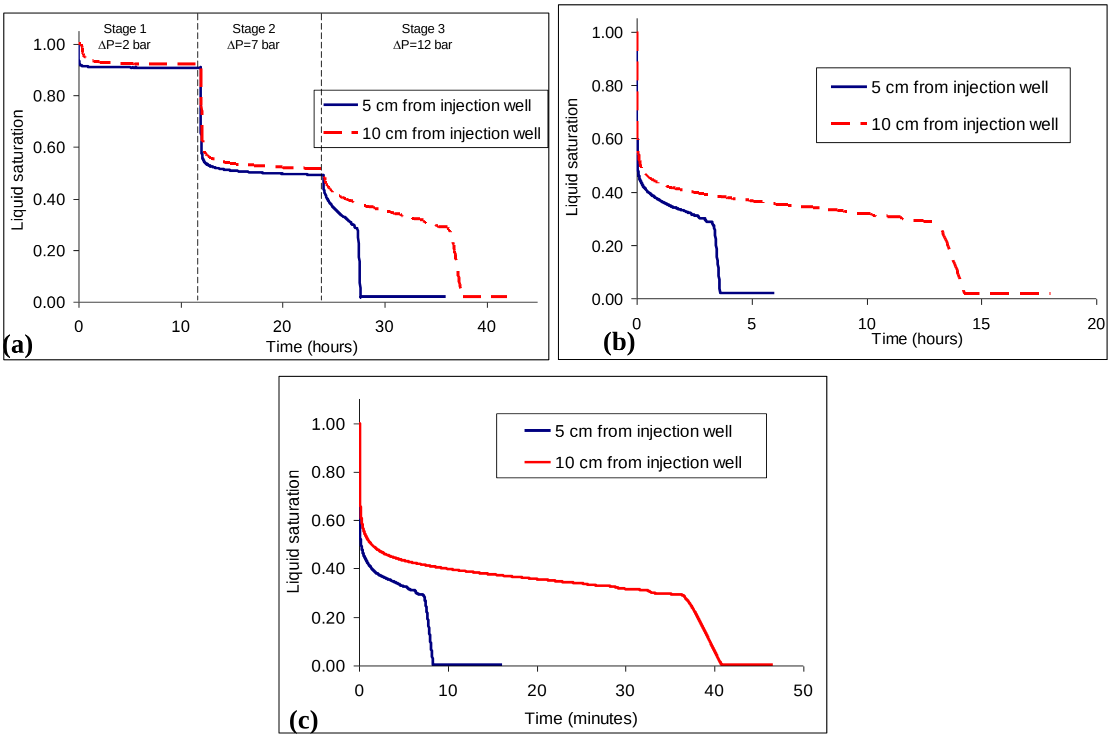

Figure 8 Variation of water content around the well: (a) CO_2 injection by stages; (b) massive CO_2 injection rate with an abrupt ΔP = 12 bar; (c) massive CO_2 injection rate with an abrupt ΔP = 24 bar.

From these three scenarios, it is expected that the same amount of evaporated water will provide the same amount of precipitated salt. However, the numerical results indicate that the amount of salt precipitated in the scenario 3 is 5-times lower than in the two other scenarios (Table 1).

Table 1 Amount of precipitated salt in the cell located at 5 cm from the injection well.

	Amount of precipitated salt (g)
Scenario 1	5.9
Scenario 2	6.4
Scenario 3	0.9

This difference is probably due to capillary effects. When the injection flow rate is sufficiently high (scenario 3), the capillary effects are reduced by the convection flow rate. No capillary water flow can go against the major gas flow and only residual water is evaporated. In the two other scenarios (1 and 2), a capillary water flow operates against the main gas flow feeding the evaporated cells with “new” fresh brine. Consequently, the amount of evaporated water is higher than the residual water providing more important amounts of precipitated salts.

This point is particularly interesting: the amount of salt deposits due to water evaporation does not depend only on the initial salinity of pore brine. It is also dependent on the injection flow rate and the capillary characteristics of the rock. A good estimation of rock characteristics and in particular of capillary properties is needed to thus define the adequate injection flow rate minimizing the precipitation risks.

5. Conclusions

Drying processes are investigated through laboratory experiments and numerical simulations to evaluate the dynamic of the water saturation decrease in sandstone and the consequences of induced salt depositions on the injectivity.

We demonstrate that in porous media of low permeability, the relative permeability of gas phase significantly increases when water saturation is lower than the residual liquid phase saturation. But, when this parameter is adjusted, the numerical code is able to reproduce the drying time and the outlet gas flow rate measured at laboratory scale on cores, using a two-phase Darcy flow and thermodynamic equilibrium between phases. The determined parameters are not temperature-dependent, for explored conditions, and they can be used at various temperatures. For rocks with higher permeability, this modification of relative permeability curves is not necessary. The code can represent the evolutions of water content in cores with a good accuracy.

At field scale, the rocks characteristics defined at laboratory scale are used to predict the behaviour of the near-well zone according to the injection gas flow rate. We demonstrated that the precipitation process and the amount of salt deposits are related to different parameters:

- *the salinity of the initial brine*: the more concentrated the brine is, the more massive the salt deposit is;
- *the residual water content*: water entrapped in pores is evaporated by gas injection. The higher this content is, the more important the amount of precipitated salt is;
- *the gas injection flow rate and the capillary forces within the system*: the numerical calculations show that the capillary properties of the rock prevent a sudden evaporation of the irreducible water by continuously feeding the injection zone with “new” brine coming from reservoir zones distant from the injection well. But, a gas injection rate sufficiently high can reduce the capillary forces and then limit the precipitation of salts close to the injection well.

All these parameters have to be known (and defined) in order to improve the management of the long-term injection of CO_2 in the saline aquifers.

Acknowledgements

This work was carried out within the framework of the “Proche Puits” project, co-funded by the French National Agency for Research (ANR).

References

[1] André, L., Audigane, P., Azaroual M., Menjoz A., 2007. Numerical modeling of fluid-rock chemical interactions at the supercritical CO_2-liquid interface during supercritical carbon dioxide injection into a carbonated reservoir, the Dogger aquifer (Paris Basin, France). Energy Conversion and Management, 48, p. 1782-1797.

[2] André L., Azaroual M., Menjoz A., 2010. Numerical Simulations of the Thermal Impact of Supercritical CO_2 Injection on Chemical Reactivity in a Carbonate Saline Reservoir. Transport in Porous Media, 82(1), p. 247-274.

[3] Peysson Y., Bazin B., Magnier C., Kohler E., Youssef S., 2010. Permeability alteration die to salt precipitation driven by drying in the context of CO_2 injection. International Conference on Greenhouse Gas Technologies (GHGT-10), Amsterdam, 19-23 September 2010.

[4] Mahadevan J., 2005. Flow-through drying of porous media. PhD Dissertation. The University of Texas at Austin.

[5] Mahadevan J., Sharma M.M., Yortsos Y.C., 2007. Water removal from porous media by gas injection: experiments and simulation. Transport in Porous Media, 66, p. 287-309.

[6] Kleinitz W., Dietzsch G., Köhler M., 2003. Halite scale formation in gas producing wells. Chemical Engineering Research and Design 81 (PartA).

[7] Zeidouni M., Pooladi-Darvish M., Keith D., 2009. Analytical solution to evaluate salt precipitation during CO_2 injection in saline aquifers, International Journal of Greenhouse Gas Control, 3, p. 600–611

[8] Pruess K., Oldenburg C.M., Moridis G.J., 1999. TOUGH2 User’s Guide, Version 2.0. Lawrence Berkeley National Laboratory Report LBNL-43134, Berkeley, CA (USA).

[9] Oldenburg C.M., Moridis G.J., Spycher N., Pruess K., 2004. EOS7C Version 1.0: TOUGH2 Module for Carbon Dioxide or Nitrogen in Natural Gas (Methane) Reservoirs. Lawrence Berkeley National Laboratory Report LBNL-56589, Berkeley, CA (USA).